



THE ADAPTABILITY OF DISCRETE ELEMENT METHOD (DEM) IN AGRICULTURAL MACHINE DESIGN

Author(s):

Á. Kovács – K. Kotroczy – Gy. Kerényi

Affiliation:

Department of Machine and Product Design, Budapest University of Technology and Economics, Műegyetem rkp. 3., Budapest, H-1111, Hungary

Email address:

kovacs.adam@gt3.bme.hu, kotroczy.krisztian@gt3.bme.hu, kerenyi@eik.bme.hu

Abstract

This study focuses on the adaptability of discrete element method (DEM) in agricultural machine design.

Laboratorial three point bending, compression and dynamic cutting tests were conducted to define the main mechanical parameters and behaviour of corn stalks.

For the DEM simulations of the laboratorial tests Timoshenko-beam bonded model was selected. With modifications of the geometry structure and the input parameters of the contact model, during an iteration process, the right assembly was found.

The findings of the study clearly demonstrate that DEM capable of simulating the interactions, among the plants, the parts of the machine, and the appeared loads during agricultural processes.

Keywords

DEM, maize, stem, agricultural machine design

1. Introduction

The increasing demand for high-quality agricultural products presents a big challenge for the developers of agricultural machinery. Due to the seasonal nature of agricultural products in situ tests of new constructions are limited in time and often prove to be very expensive. In the field of agricultural machine design numerical methods are not available which could properly replace field tests.

The utilization of corn plants and crops is remarkable worldwide, the corn production in the world is almost 1000 million tons. In 2014 almost 10 million tons of corn were harvested by farmers in Hungary (HCSO, 2015), which demonstrates the significance of the plant in the agriculture of the country.

This study focuses on the adaptability of discrete element method (DEM) in agricultural machine design in connection with maize product.

The paper builds around a literature review on the industrial or agricultural applications of the discrete element method. DEM is used to investigate bulk agricultural materials widely.

Kepler et al. calibrated the micromechanical parameters of a sunflower DEM model based on odometer tests so that the model can sufficiently approach the macro mechanical behaviour of the

real bulk material. [1.] Földesi et al. investigated the pressure relations of an oil press by DEM simulations. [2.] Tamás et al. examined the soil-tool interaction and the relations in cohesive soil by using the DEM [3.].

In connection with string materials fewer literature can be found. Kemper et al. investigated the iteration among grass stalk and rotation mower by DEM [4.].

To calibrate a DEM model, in situ and laboratorial test are indispensable. Qin Tongdi et al. investigated the effect of different production fields on three point bending behaviour of the same maize species [5.]. Sun Zhong-Zhen et al. examined the effect of moisture content on three point bending behaviour of maize stalks [6.]. M. Azadbakht et al. accomplished in situ dynamic cutting test by a modified Charpy impact test to analyze the resistance against dynamic cutting force of maize stalks [7.].

Based on the findings, the agricultural product (maize) and its typical loads (compressive, three point bending loads and dynamic cutting) were determined giving the research a more concrete and better focus.

2. Material and methods

Discrete element method (DEM) is developed to investigate bulk materials which contains separate parts. The definition of a DEM model is the following [8]: It contains separated, discrete particles which have independent degrees of freedom and the model can simulate the finite rotations and translations, connections can break and new connections can come about in the model.

Based on harvest and product processes of mature maize stalks the main loads of the stalk were determined. Root, leaves and ears of the plant were neglected in our study. First of all the physical properties of the stalks (mass, length, diameter, shape) were measured and noticed. After that laboratorial three point bending, compression and dynamic cutting tests were conducted to define the main mechanical parameters and behaviour of corn stalks.

The examination of the available contact models was the first step of the modelling. After that the models were compared and the Timoshenko-beam bonded model, which is based on the Timoshenko-beam theory, was selected for the study.

In the next step the possible DEM geometry formations of the real plant geometry was analysed. To select the right geometry model that can simulate the mechanical and physical properties and behaviour of the plant most accurately, DEM simulations of the laboratorial tests were conducted.

With modifications of the geometry structure and the input parameters of the contact model, during an iteration process, the right assembly was found.

3. Measures

For the measures the maize stalks were divided in determined parts. The first node above the air root was marked 1st node and after the first node the first internode was marked 1st internode. Following this logic the entire stalk was divided as seen on Figure 1.

Before each measure the necessary specimens were prepared. During the preparation leaves and ears were pruned from the stalk and after that the necessary physical parameters were measured. Finally the stalks were cut to the right size for the mechanical measures.

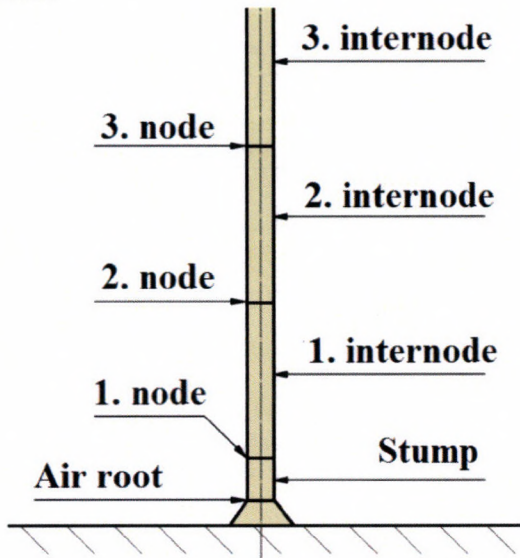


Figure 1. Dividing of the maize stalks

Analyses were conducted for the first internode so hence the results of the study are in relation to the first internode.

During the measurement of the physical parameters 8 plants were investigated. Moisture content, diameter, length and mass of the first internode were measured (Table 1.).

Table 1. Physical parameters of the first internode

Parameters	Results
Average moisture content	64,67 %
Average diameter	24,80 mm
Average length	120,63 mm
Average mass	42,52 g

The aim of the three point bending test was to define the resistance against bending of the first internode. During the measure a zero point was defined by touching the specimen with the bending tool. Then the crosshead of the machine was moved with 200 mm/min to 50 mm displacement. Five specimen were measured, the results were calculated with statistical methods from the measured data (Figure 2.) in order to calibrate the DEM model of the first internode. The bending diagram has three different sections: the linear section where the relation is linear among the force and displacement, the contraction section where the diagram reaches the maximum force and the bended cross-section of the internode is flattening, and finally, the plastic joint section where the bended cross-section is crashed so the resistance against the bending is decreasing gradually until the end of the bending test.

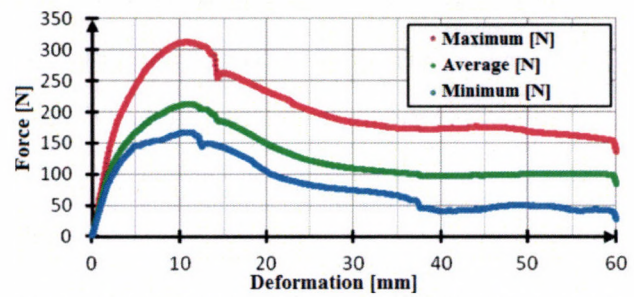


Figure 2. Three point bending test results of the first internode

The aim of the compression test was to determine the side pressing resistance of the first internode and the crossway and residual sideways deformation over the stalk length. After the prepared specimens were placed in the clamp jaws the crosshead of the machine compressed them with 100 mm/min pace. Five specimens were measured, the aim of the evaluation was to determine an average deflection - resistance force diagram to calibrate the DEM model of the first internode (Figure 3.).

On this figure two different sections can be observed: the constant section which goes up to 30% deflection where the resistance force is close to constant, the exponential section that goes from 30% to 75% deflection where the resistance force is exponentially increasing.

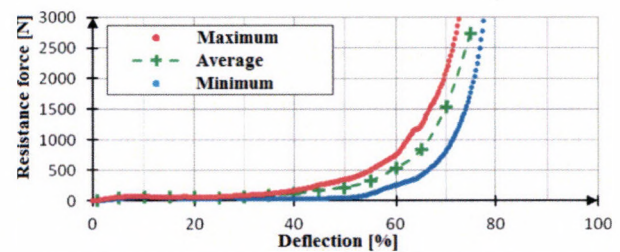


Figure 3. Compression test results of the first internode

The aim of the dynamic cutting test was to determine the cutting work of the first internode. A Charpy impact test was revised for the measurement by a special cutting blade and fixing apparatus (Figure 4.). The position of the gripper and the cutting apparatus was adjusted to minimize the gap among the cutting edge and the fixing apparatus. After a specimen was fixed the test was carried out with 3,47 m/s cutting speed. Five specimens were investigated, and based on the evaluation of the results the average cutting work was 17,57 J.

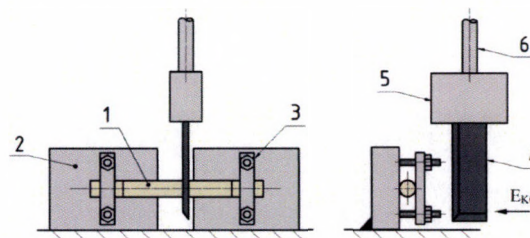


Figure 4. Sketch of dynamic cutting test (1: Measured sample 2: Stalk gripper 3: Fixing unit 4: Cutting blade 5: Blade gripper 6: Flywheel arm)

4. Physical model of corn stalk

In the geometry model of the first internode the following neglects were used: the shape of cross-section was a standard circle instead of an ellipse, over the length of the internode the

size of the cross-section was constant, any other special feature of the internode was also neglected.

The smallest unit of the DEM geometry model is the particle. Basically this unit in the EDEM 2.7 software has a sphere shape but any special shapes can be created through the combination of the different spheres. For a better distribution of the external loads the shape of the bark was chosen for a cylinder that is made up by two sphere shapes (Figure 5. a.). For determining different cross-sections in the pith simple spheres were used (Figure 4. b.).

The size of the particles were based on the measured size of the plant and the geometry structure of the DEM geometry. The radius of the spheres was chosen for $r=2,57623$ mm in consideration of the high accuracy.

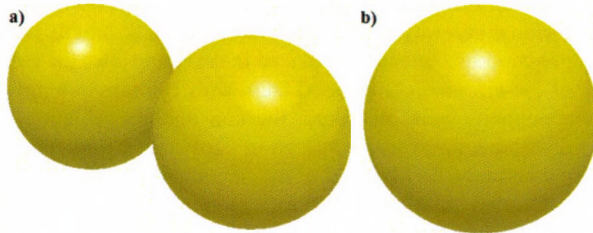


Figure 5. a) Shape of the particles in the bark b) Shape of the particles in the pith

The second largest unit of the geometry is the module that consists of a couple of particles in a determined structure (Figure 6.). The particles of the bark (light and dark green particles) have a special offset structure similar to a fastener to better disperse the external loads to the particles of the pith. The particles of the pith (yellow and orange particles) formed segregated cross-sections side by side.

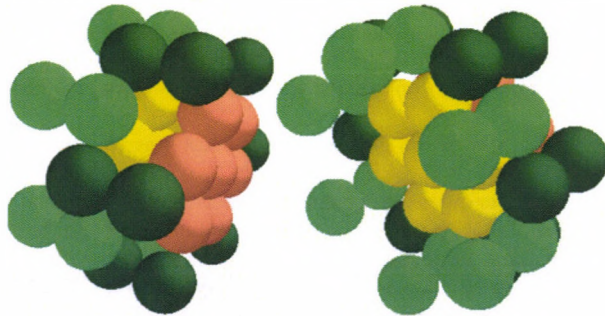


Figure 6. The geometrical structure of a module

The complete geometry model of the internode, which represents a standard cylinder geometry, is built up from several modules one after the other (Figure 7.).

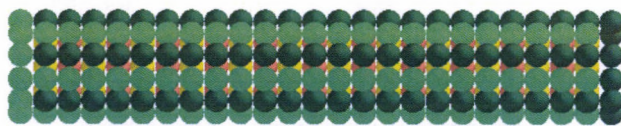


Figure 7. DEM geometry model of the first internode

5. Connection system of the model

Different connections were determined in axial and tangential directions of the bark and the pith, and another connection was defined between the pith and the bark.

The particles in the pith and in the bark have different mechanical parameters (Table 2.).

Table 2. Mechanical parameters of particles

	Particles of bark	Particles of pith
	P1&P2	P3&P3
Poisson's ratio [-]	0,25	0,25
Shear stiffness [Pa]	1,00E+08	1,00E+06
Density [kg/m ³]	2650	2650

During an interaction among the different particles of the stem or among the particles and the parts of the geometry special connection parameters were defined (Table 3.).

Table 3. Mechanical parameters of interactions

	Among particles of stem	Among particles of stem and geometry
Coefficient of friction [-]	0,3	0,3
Coefficient of rolling friction [-]	0,01	0,01
Coefficient of restitution [-]	0,5	0,5

In the bark in tangential (P1:P2) and axial direction (P1:P1 & P2:P2) different connections were defined to simulate the different behaviour of the stalk in these directions. (Figure 8.) (Table 4.).

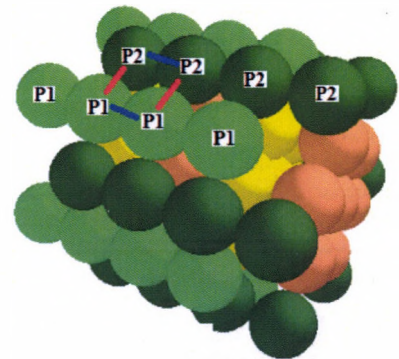


Figure 8. Connection model of the bark

Table 4. Mechanical parameters of connections among the particles of bark

	P1:P1 P2:P2	P1:P2
Coefficient of damping [-]	0,5	0,5
Young-modulus [Pa]	1,00E+08	1,00E+08
Poisson's ratio [-]	0,15	0,15
Max. compression stress [Pa]	7,50E+06	3,75E+06
Max. tension stress [Pa]	10,00E+06	5,00E+06
Max. shear stress [Pa]	5,00E+06	2,50E+06
Coefficient of variation [-]	0	0
Radius multiplier [-]	1,00	1,00

In the pith in tangential (P3:P3 and P4:P4) and axial direction (P3:P4) similar different connections were defined to simulate the different behaviour of the stalk in these directions. (Figure 9.) (Table 5.).

For the better load distribution in the model a connection was defined among the particles of the pith and the bark (P1:P3; P2:P3; P1:P4; P2:P4) (Figure 9.) (Table 6.).

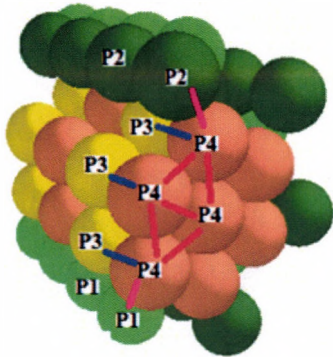


Figure 9. Connection model of the pith

Table 5. Parameters of connections among the particles of pith

	P3:P4	P3:P3 P4:P4
Coefficient of damping [-]	0,5	0,5
Young-modulus [Pa]	1,00E+07	1,00E+06
Poisson's ratio [-]	0,15	0,15
Max. compression stress [Pa]	2,00E+07	1,00E+04
Max. tension stress [Pa]	3,00E+07	1,00E+06
Max. shear stress [Pa]	1,50E+07	5,00E+05
Coefficient of variation [-]	0	0
Radius multiplier [-]	1,00	0,50

Table 6. Parameters of connections among the particles of pith and bark

	P1:P3 P2:P3 P1:P4 P2:P4
Coefficient of damping [-]	0,5
Young-modulus [Pa]	1,00E+08
Poisson's ratio [-]	0,15
Max. compression stress [Pa]	1,30E+07
Max. tension stress [Pa]	2,00E+07
Max. shear stress [Pa]	1,00E+07
Coefficient of variation [-]	0
Radius multiplier [-]	0,50

6. Results

The model was evaluated with quantitative and qualitative evaluation methods. With the quantitative method the real measure diagrams were compared with the simulation diagrams.

With the qualitative method cross-section deformations, crashes, breaks of the model were compared with the measured experiences of the real specimens.

The result from the three point bending simulation test is shown on Figure 10. The sudden changes of the diagram came from the DEM geometry, because the sudden connection breaks and sudden movements of the particles resulted in the observed changes on the chart. From this reason a sixth grade polynomial trend line was fitted on the results to correct the sudden changes (Figure 10). The simulated results are between the minimal and maximal results of the measure. The linear section, the contraction section and the plastic joint section of the simulation data approached the measured data very well.

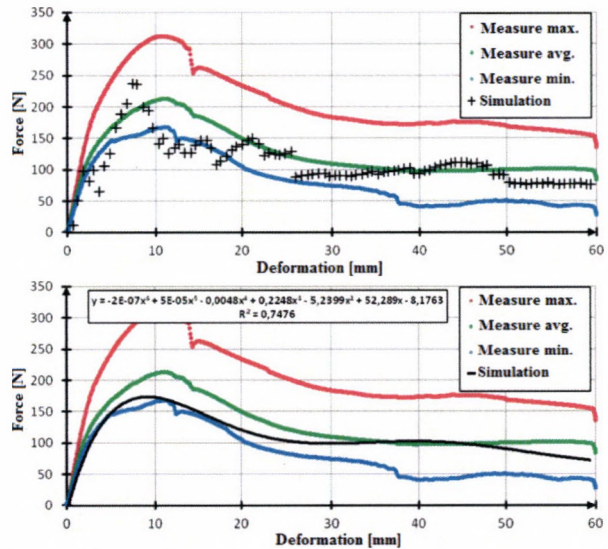


Figure 10. Results of three point bending test simulation

The simulation data of the compression test are above the measured data of the real specimens (Figure 11.). To fit an exponential trend line it was necessary to create an average point of the gradually increasing sections of the data. These data approach the measured data from above up to 60% deflection, then a nearly vertical section of the chart can be observed that is sharper than the measured characteristic.

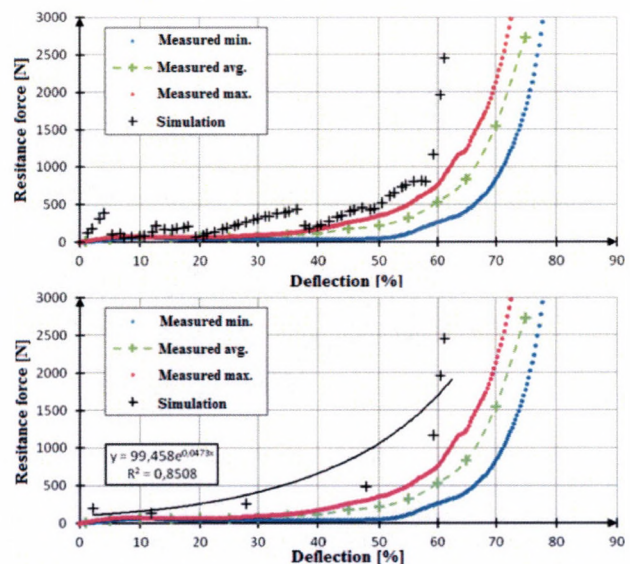


Figure 11. Results of compression test simulation

The simulation result of the dynamic cutting is a cutting force – time chart as opposed to the results of the measures (Figure 12.).

To compare the different results the area, that is limited by the data points, was calculated by the classic trapeze integration rule and was multiplied by the constant cutting force (3,47 m/s). The simulated dynamic cutting work was 19,15 J, so the difference from the measured results is only 9%, which is a very good accuracy.

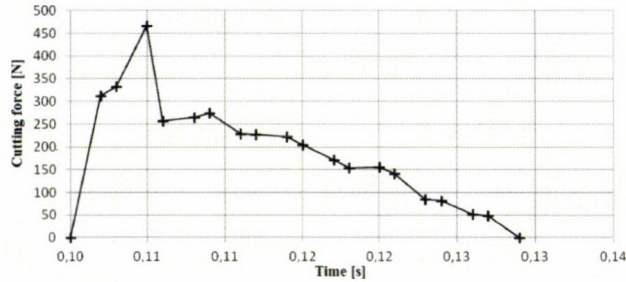


Figure 12. Result of dynamic cutting simulation

During the qualitative evaluation of the three point bending moment the deformation of the cross-section under the bending edge and the residual deformation were analyzed.

The bended cross-section deformation of the model approaches the real deformation of the internode very well, however the simulated deformation is less than the real deformation (Figure 13.).

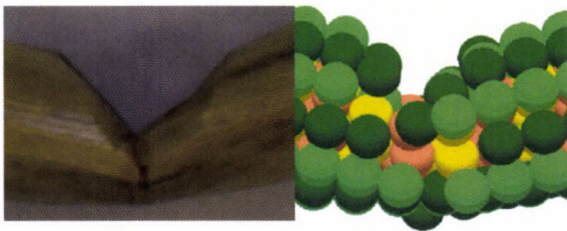


Figure 13. The real and simulated bended cross-section deformations

The residual deformation of the model approaches the real deformation of the internode well, but the simulated internode is damaged during the simulation (Figure 14.). The right side of the simulated internode was cracked in axial direction and thanks to this the threads of the pith appeared. This phenomenon wasn't observed during the measures.

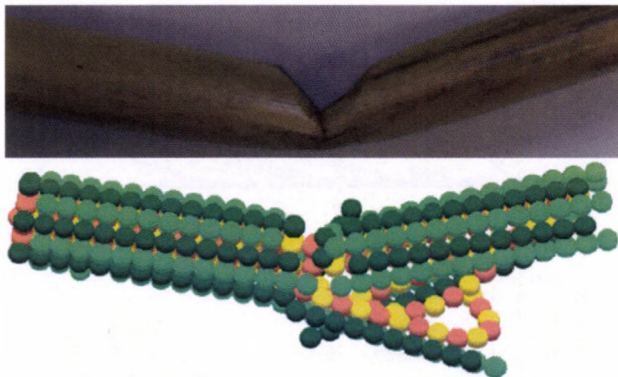


Figure 14. The real and the simulated residual deformations

During the qualitative evaluation of the compression test the deformations and the damages of the cross-section were analyzed.

The deformation and condition changes of the simulated internode appeared earlier during the compression process and

were more effective (Figure 15.). On the first picture the initial conditions can be observed. On the second figure the deformation of the simulated internode is bigger than the real observed but the crashed condition of the two samples is the same. On the last figure huge deformations can be noticed in connection with both internodes, but the crashed condition of the simulated sample is completely different. During the real compression test the bark is still embracing the pith during the whole test, but in the simulation the bark is crashed and from this reason the geometry structure completely broke and the functions of the bark were lost. In this case the behaviour of the model internode during the compressing test is still acceptable.

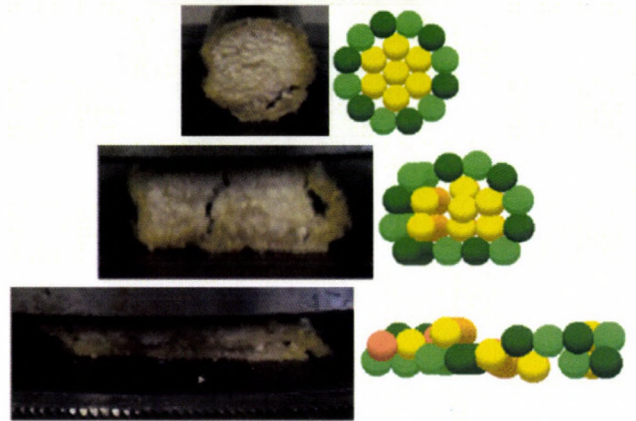


Figure 15. The real and simulated compression process of the first internode

During the qualitative evaluation of the dynamic cutting test the cutting surface was analyzed.

Due to the geometry structure of the model (fastener structure of the bark) the perfectly flat cutting surface cannot be expected. Even so the simulated cutting surface converged the real surface very well (Figure 16.). The threads of the bark show crashed behaviour similar to the real internode and the pith demonstrate a perfectly flat, straight cutting surface. Thanks to the structure of the bark several particles flew off due to the strong impact.

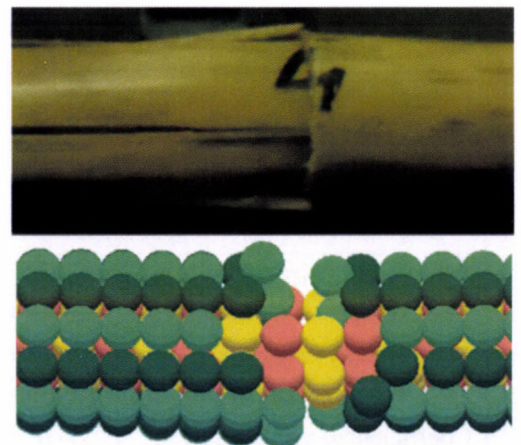


Figure 16. The real and the simulated cutting surface

5. Conclusion

The DEM model of the first internode, which is based on the Timoshenko beam theory, showed reassuring results in connection with the three point bending, compression and dynamic cutting test. The quantitative and qualitative evaluations

clearly demonstrate that the discrete element method (DEM) is capable of simulating the interactions, among the plants, the parts of the machine, and the appeared loads during agricultural processes.

To increase the accuracy of the simulations a viscous-elastic connection model is essential to simulate the real relations between the stress and strain conditions and the changing of the Young-modulus during the simulations.

Acknowledgements

We would like to thank Katalin Gaál from the Institute of Agricultural Engineering at Gödöllő, Dr. Gábor Szabó from the Department of Polymer Engineering at BUTE, Dr. Imre Obrulov from the Department of Material Science and Engineering at BUTE and Dr. Tibor Poós from the Department of Building Services and Process Engineering at BUTE for their valuable and constructive help.

References

- [1.] **Kepler I., Kocsis L., Oldal I., Csatár A.:** 2011. Determination of the discrete element model parameters of granular materials, *Hungarian Agricultural Engineering*, No 23/2011, pp.30-32, HU ISSN 0864-7410
- [2.] **Földesi B., Rádics J. P., Tamás K., Jóri I. J.:** 2011. Determining pressure relations of vegetable oil press using discrete element method simulation, *Hungarian Agricultural Engineering*, No 23/2011, pp. 33-36, HU ISSN 0864-7410
- [3.] **Tamás K., Jóri. J. I.:** 2011. 2D DEM simulation of the soil-tool interaction in cohesive soil, *Hungarian Agricultural Engineering*, No 23/2011, pp. 45-49, HU ISSN 0864-7410
- [4.] **S. Kemper, T. Lang, L. Frerichs.:** 2014, The overlaid cut in a disc mower – results from field tests and simulation, *Landtechnik* 69(4), pp. 171-175, ISSN 0023-8082
- [5.] **Tongdi Q., Yaoming L., Jin C.:** 2011. Experimental study on flexural mechanical properties of com stalks, *New Technology of Agricultural Engineering (ICAE)*, 2011 International Conference on. pp. 130-134, <http://dx.doi.org/doi:10.1109/ICAE.2011.5943766>
- [6.] **Zhong-Zhen S., Huan-Xin J., He-Ping C., Qiu-Sheng Y., Li-Xin L., Li W., Guo-Lin C.:** 2013. The Viscoelasticity Model of Com Straw under the Different Moisture Contents, *Mathematical Problems in Engineering*, Volume 2013, <http://dx.doi.org/doi:10.1155/2013/320207>
- [7.] **M. Azadbakht, E. Esmailzadeh, M. Esmaili-Shayan.:** 2015. Energy consumption during impact cutting of canola stalk as a function of moisture content and cutting height, *Journal of the Saudi Society of Agricultural Sciences*, Vol. 14, Issue 12, pp. 147-152. <http://dx.doi.org/doi:10.1016/j.jssas.2013.10.002>
- [8.] **Cundall P. A., Hart R. D.:** 1992: Numerical modelling of discontinua. *Engineering Computations*, Vol. 9, Issue 2, pp. 101-113. <http://dx.doi.org/10.1108/eb023851>